JOURNAL OF MATERIALS SCIENCE 25 (1990) 3864-3874

Interphase phenomena in silicon carbide single filament composites

YVES MANIETTE, A. OBERLIN
Laboratoire Marcel Mathieu, 2 avenue du Président P. Angot, 64000-Pau, France

A heat-treated SiC Nicalon NLP 201 fibre and four single-filament composites have been characterized by means of transmission electron microscopy techniques. Phenomena occurring before and during the chemical vapour deposition process have been investigated. First, the thermal decomposition of the fibre is explained. The SiC microcrystals which are in the fibre decompose giving a solid carbonaceous porous residue and a gas phase containing mainly silicon. A catalytic reaction is noticed. This reaction explains the reorganization of carbon when silica is present. Another reaction between silica and carbon, giving rise to the formation of SiC, also explains the formation of an SiC interphase when depositing a carbon matrix. The non-stability of the SiC Nicalon fibre explains all of these transformations, the major consequence of them being a decrease in its mechanical properties when used in a composite material.

1. Introduction

The interphase phenomena in silicon carbide composite materials were studied. It is now well known that the resilience of such bulk composite materials is controlled by the pull-out phenomena which may occur when they are loaded. These phenomena are obviously due to the nature of the bonding between fibre and matrix, i.e. the interphase. Hence, physicochemical reactions occurring during the chemical vapour deposition (CVD) process must be well understood and controlled.

Nevertheless, an understanding of these reactions is not easy when the sample is a bulk composite. For this reason, single-filament composites (i.e. coated fibres) have been made and mechanically characterized [1]. This previous study showed that a "matrix effect" may occur. This effect, which is not yet understood, reduces the apparent mechanical strength of the fibre. In order to understand this effect, transmission electron microscope (TEM, Philips EM400, 120 kV) studies have been carried out on such samples.

2. Sampling

Four single-filament and a heat-treated single filament have been studied. Table I gives details of those samples.

3. Techniques

3.1. Preparation

Microtomy has been used to obtain samples as thin as about 50 nm. An improvement of the microtomy technique was necessary. This improvement is based on the slicing of a bevel-ended single filament composite, as described in another paper [2].

3.2. Transmission electron microscopy

Owing to the fact that the main zones of interest in the interphases may be as thin as a few nanometres, TEM is a convenient technique for studying them. The resolution can be 0.14 nm in the lattice fringes or 0.6 nm in the dark-field conditions we used.

The four main techniques of high-resolution TEM have been used: bright-field (BF), dark-field (DF), selected area electron diffraction (SAD) and lattice fringes (LF). These techniques, applied to the study of a mixture of carbon and silicon carbide phases, have already been precisely described [3–6]. The capabilities of these techniques are listed in Table II.

4. Results

4.1. Low-pressure heat-treated fibres

This sample was prepared using the conventional microtomy technique. Despite the fact that the sample often broke, some particles remain fastened to the embedding medium. Obviously these particles issued from the most external part of the sample, i.e. the surface. Such a particle has been studied and is shown in Figs 1a to d.

4.1.1. DF study

Figs 1c and d are two SiO_2–C_{002} DF micrographs showing the carbon-layer stacks oriented parallel to the double bars. The micrographs show that the first

TABLE I Sampling

Sample	Fibres	Matrix thickness (μm)	Heat treatment
1	NLP 201	None	5 h, 1000° C, low-pressure, inert gas
2	NLP 201	Carbon, 0.4	None
3	NLP 201	Carbon, 2	None
4	NLP 201	SiC, 1	None
5	NLP 201	SiC, 3	None

0022–2461/90 $03.00 + .12

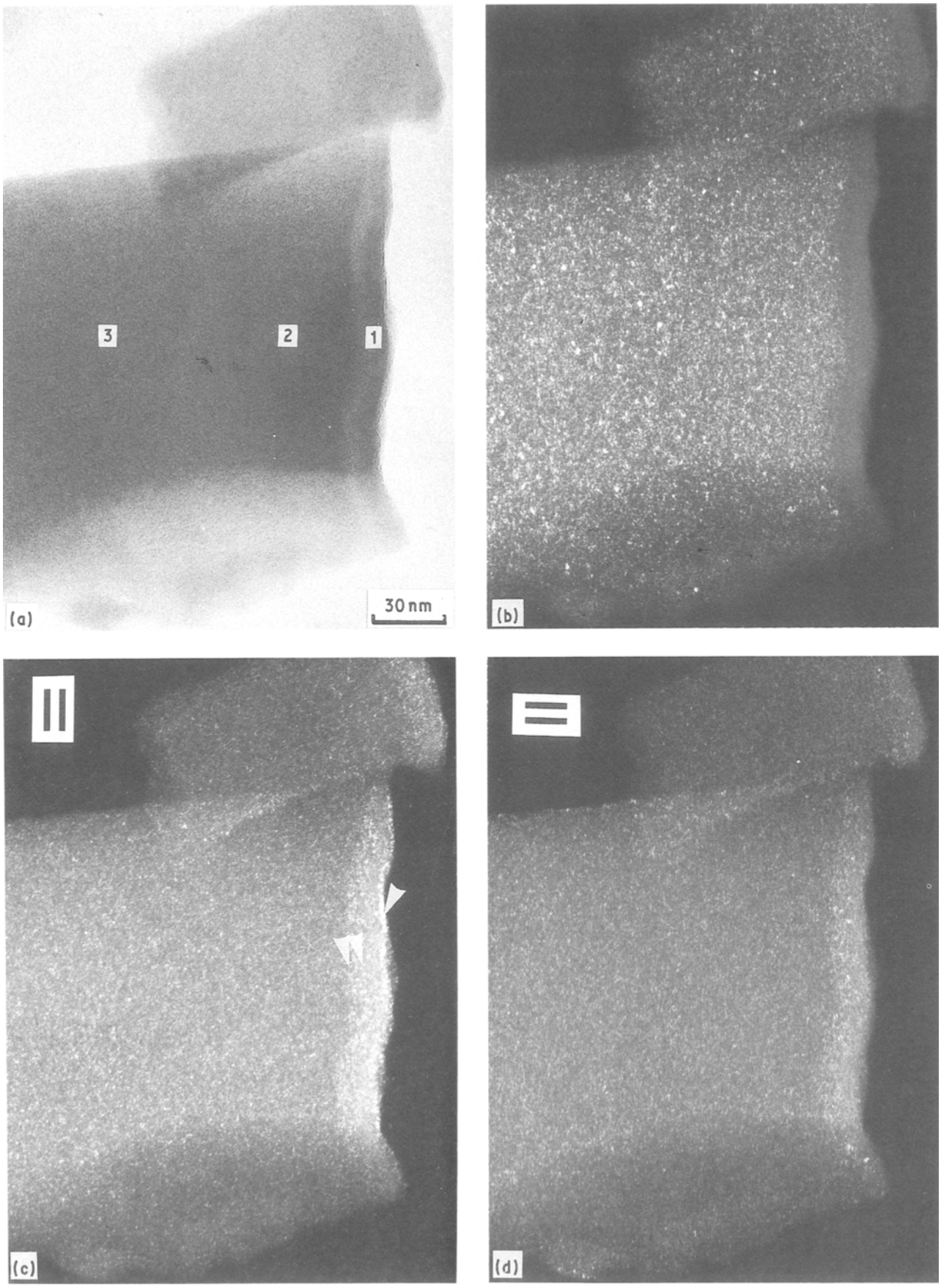

Figure 1 Nicalon NLP 201 heat treated at 1000° C, 5 h under reduced pressure (a) BF, (b) SiC_{111} DF, (c) and (d) orthogonal SiO_2–C_{002} DF.

zone, (marked 1 in Fig. 1a), which is the fibre surface, is made up of several sheets.

(a) The arrow on Fig. 1c indicates a brilliant rim which has disappeared in Fig. 1d. Hence this rim is oriented parallel to the fibre surface, and is made of carbon.

(b) Beneath this rim is a zone which is uniformly greyish when observed on the microscope screen. It shows a peculiar phenomenon which explains this greyish aspect: small scattering domains appear on the screen but their place and orientation change continuously. This phenomenon has already been studied

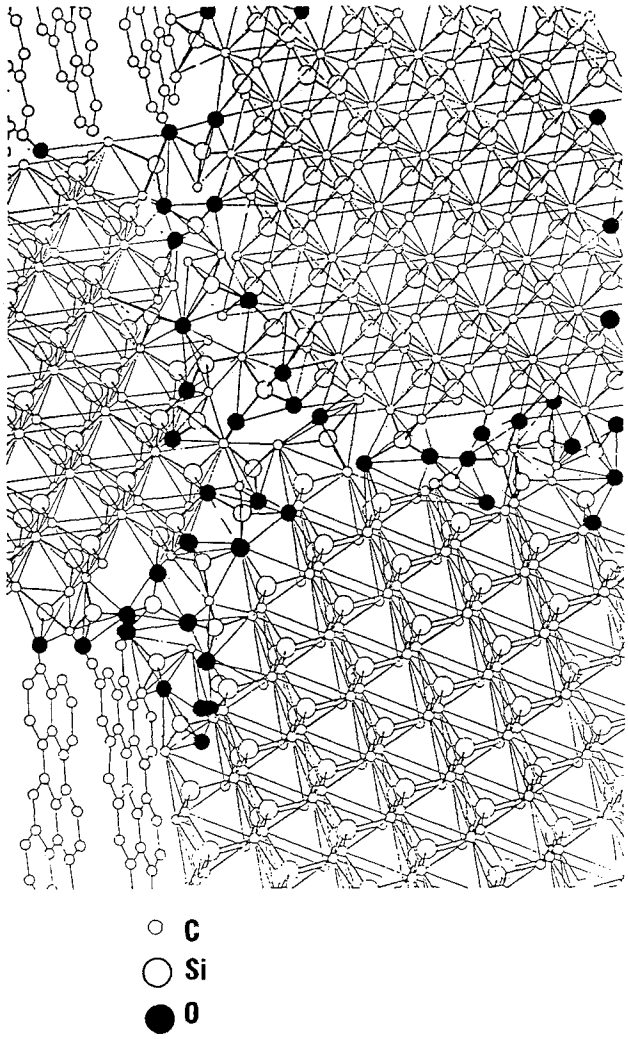

Figure 2 Model of the SiC Nicalon fibre microstructure (from [8]).

by Chaudhari [7] who showed that it is characteristic of amorphous silica. The aspect of this zone is obviously the same in both Figs c and d DF micrographs.

(c) Beneath this amorphous silica phase is another layer (double arrow) which shows an improvement of the carbon signal. The Fig. 1b, which is an SiC_{111} DF micrograph explains that this phase is not made of crystallized silica, because crystallized silica gives an intensively diffracted beam near that of SiC_{111}. As a consequence, if this phase was made of crystallized silica, it would be visible on Fig. 1b DF. On the contrary, we notice a complete disappearance of the diffraction units at this point.

Beneath this carbon-containing phase is another phase (zone 2) made of small SiC crystals, about 1 nm in size, mixed with carbon stacks of the same size.

There is a gradient in the SiC crystal size when approaching zone 3, throughout which their size is up to 3 nm. No gradient is seen in the carbon layer stack grain size.

TABLE II Capabilities of TEM techniques

Technique	Capabilities
SAD	Obtains the diffraction pattern of an area as small as about 1 μm diameter
DF	Obtains the images of coherent domains as small as 0.6 nm, knowing precisely their orientation with respect to the sample. In practice it is possible to image selectively carbon, silicon carbide and amorphous or crystallized silica
LF	Obtains a highly magnified image of the lattice planes, seen edge-on. The resolution (line resolution) is 0.14 nm. The microtexture of carbon (0.335 nm spacing) and silicon carbide (spacing = 0.251 nm) can be clearly determined

4.1.2. Discussion

The microstructure of zone 3 resembles that of the NLP 201 SiC fibre. This microstructure has already been described previously [4] and has been sketched by other authors [8] using several techniques (Fig. 2).

The important result which has been found during this study concerns the structural transformation of the fibre near its surface. Fig. 3 shows this transformation and clearly indicates the several phases which are to be found beneath the surface of the sample. This succession of phases may be understood by remembering the behaviour of SiC when exposed to high temperatures. It has now been noticed many times [9–12] that SiC decomposes below 1000° C according to the reaction SiC → Si + C. Through this reaction silicon vaporizes and a graphitic carbon phase remains on the surface [13]. Muelhoff *et al.* [13] showed that the reaction began at 627° C (or between 600 and 650° C) and computed the vaporization rate of silicon at 1000° C. About three silicon monolayers may disappear within 5 min. Nevertheless, when studying large crystals, this phenomenon can only be noticed by LF study of the surface [14]. On the contrary, if the initial crystals are small, as is the case in this study, the disappearance of some monolayers may cause the SiC crystal to be largely reduced in size. At the same time, some small carbon layer stacks appear, the size of which is, of course, about 1 nm. These stacks are then added to those initially present. Thus, the thermal degradation of the SiC crystals, as studied on large crystals, may be applied to the nanometric crystals of the SiC fibre. The phenomenon described here explains the gradient in the SiC crystal sizes, varying from 3 nm in the bulk fibre down to 0 nm beneath the surface (Fig. 1b) where only badly organized carbon is present.

On the other hand, it is important to know how the silicon-containing vapour phase will behave. It is known that silicon may react with oxygen to produce SiO_2. At 1000° C the oxygen equilibrium partial

Fibre Centre					Surface
SiC > 2 nm +C	SiC < 1 nm +C	C	SiO_2	C	
Approximate thicknesses (nm)	80	10	20	2	oriented

Figure 3 The structural transformation of the fibre near its surface indicating the phases found.

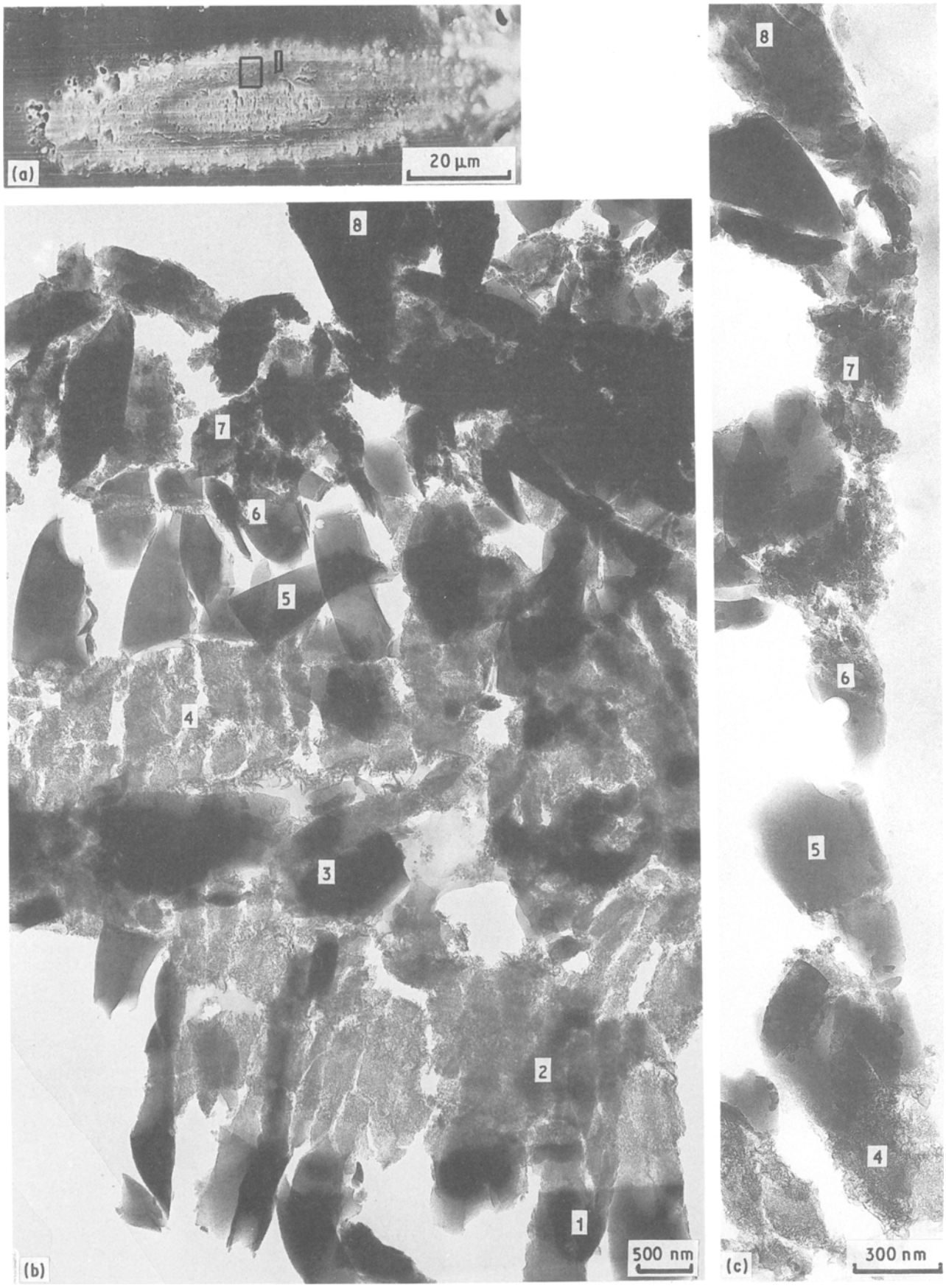

Figure 4 Single filament composite NLP 201–SiC (3 µm thick) (a) Embedded block used for thin sectioning observed by SEM. (b) and (c) BF of the interphase from 1 (intact fibre) to 8 (SiC matrix).

pressure is about 10^{-21} Pa [15]. Thus silicon issuing from the SiC crystals may react with oxygen traces contained in the furnace and to form an amorphous silica layer.

4.1.3 Conclusion

Despite the fact that the fibre is exposed to a high temperature (1300° C) during the fabrication process [16], it becomes obvious that a relatively long-term

treatment at lower temperatures under reduced pressure (1000° C) induces a structural transformation near its surface. This transformation, due to the long residence time in the CVD furnace, must be taken into account in understanding the interphase phenomena occurring during the CVD process.

4.2 The thick SiC coating (3 μm)

4.2.1 Evidence of an interphase

Fig. 4a shows a polished section (microtome block) of this sample, observed by SEM. The shape is ellipsoidal due to the orientation of the sample with regard to the diamond knife displacement. Three zones appear on this micrograph.

(a) The centre zone is the fibre and is highly emissive.

(b) The external zone is the matrix and is also highly emissive.

(c) Between these two, is a less emissive interphase which will now be described. Knowing the average diameter of the Nicalon fibres this latter is deeply corroded. The matrix corresponds to the 3 μm deposit. The intermediate zone is the corroded zone, itself being 3 μm thick.

Figs 4b and c are two low-magnification micrographs, corresponding to the frames on Fig. 4a. Several zones appear. They are: 1, the intact fibre; 2, porous carbon; 3, amorphous silica; 4, porous carbon; 5, amorphous corroded silica; 6, an SiC–C phase reacting with silica; 7, a mixture of SiC and C; 8, SiC matrix.

Figure 5 Single filament composite NLP 201–SiC (3 μm thick). Zones 1 and 2. (a) BF, (c) and (d) orthogonal SiO_2–C_{002} DF.

4.2.2. Description of the interphase

All of these zones have been thoroughly characterized by means of DF and LF techniques.

4.2.2.1. Zones 1 and 2 (Figs 5 and 6). Fig. 5a shows a bright field recorded on both zones 1 and 2, i.e. the fibre and the porous carbon. Figs 5b and c show the

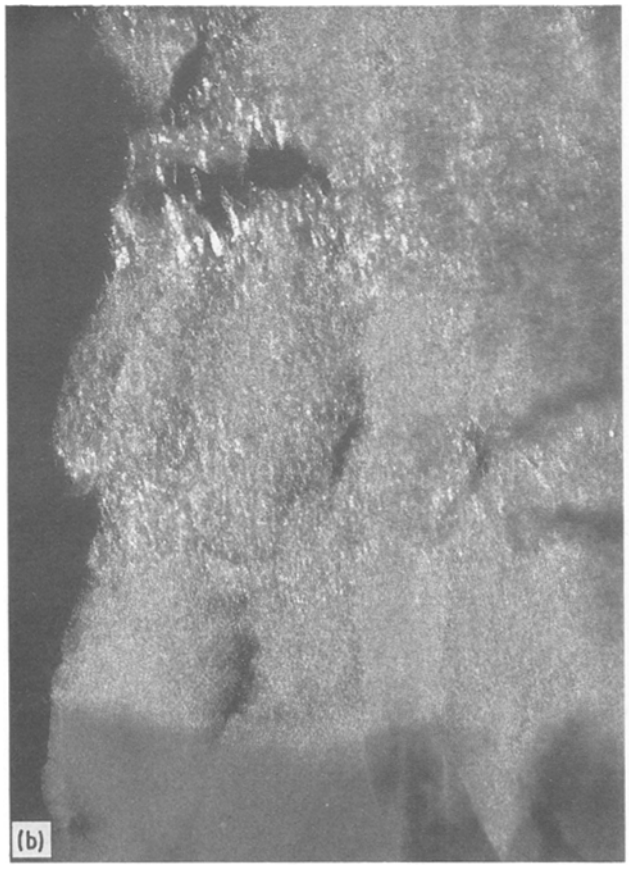

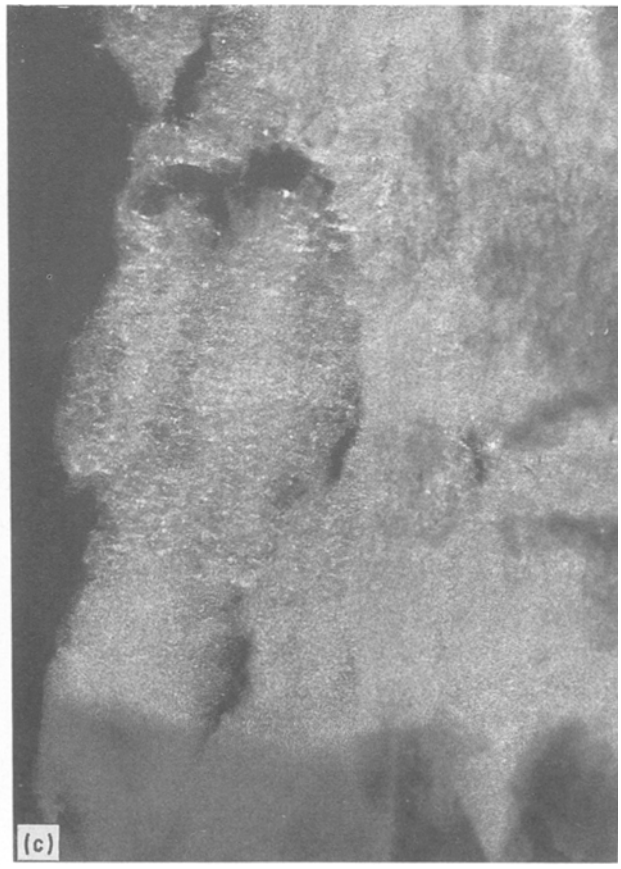

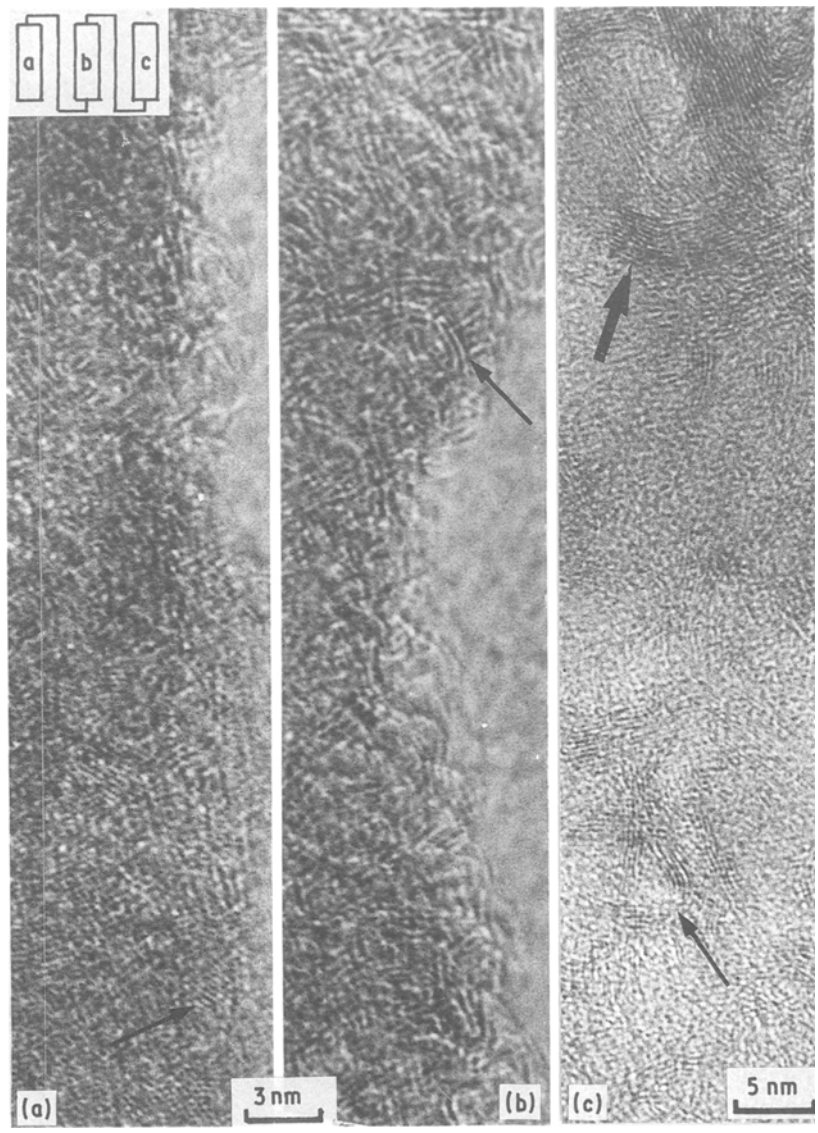

Figure 6 Single-filament composite NLP 201–SiC (3 μm thick). LF zones 1 and 2. The arrow in (a) indicates an SiC crystal. In (b) and (c) the arrows indicate carbon layer stacks.

same area recorded in diffracting SiO_2–C_{002} DF. Carbon diffracting units are small in size near the fibre at the bottom of the figures. Above, this carbon becomes better organized, in long bands showing Bragg fringes. The lattice fringe micrograph of Fig. 6 was recorded at the very limit between fibre and carbon. The three pictures were taken one above the other. The lowest part (a) shows the fibre. SiC_{111} planes can be seen (arrow) and also carbon-distorted aromatic layers. In Fig. 6b, in the middle, longer distorted carbon stacks (arrow) free of SiC can be seen. The distortions of the carbon then decrease. More perfect carbon layers can be in stacks of 10 or more, as shown in Fig. 6c (larger arrow). The microporous carbon in contact with the fibre becomes meso and macroporous.

4.2.2.2. Zone 3. The third zone is entirely made up of amorphous silica. The interface with the second zone is remarkable because of the macroporous organization of the carbon.

4.2.2.3. Zones 4, 5, and 6. The fourth zone resembles the second. The fifth resembles the third. Nevertheless specific reactions may occur between silica and carbon between zones 5 and 6. Fig. 7 shows such a reaction. Fig. 7a (BF) shows a nodule, mainly of a porous phase, enclosed in the silica phase (SAD pattern in Fig. 7d). Fig. 7b is an SiO_2–C_{002} DF. This DF allows us to recognize that the upper part of this nodule is made of macroporous carbon, organized into large bands. The SiC_{111} DF (Fig. 7c) indicates that SiC occurs everywhere between carbon and silica.

The SAD pattern, recorded on this nodule, shows the presence of both carbon and SiC (Fig. 7e).

4.2.2.4. Zones 7 and 8. Lattice fringe micrographs of these zones are shown in Fig. 8. Zone 7 is a mixture of carbon and SiC, with no orientation relationship (Fig. 8a). The last zone is the SiC matrix, made of large SiC crystals (Fig. 8b). No orientation of the SiC_{111} planes has been noticed.

4.2.3. Discussion

The main point to be noticed on this SiC-coated (3 μm) single filament is the presence of a C/SiO_2 interphase between fibre and matrix. As far as the thicknesses are concerned, we notice that this interphase thickness is as large as the coating thickness, i.e. 3 μm.

On the other hand, the microstructure of the interphase carbon must be explained. Such an organized carbon cannot be made at low temperatures (1000° C), a temperature of about 2000° C being required to get

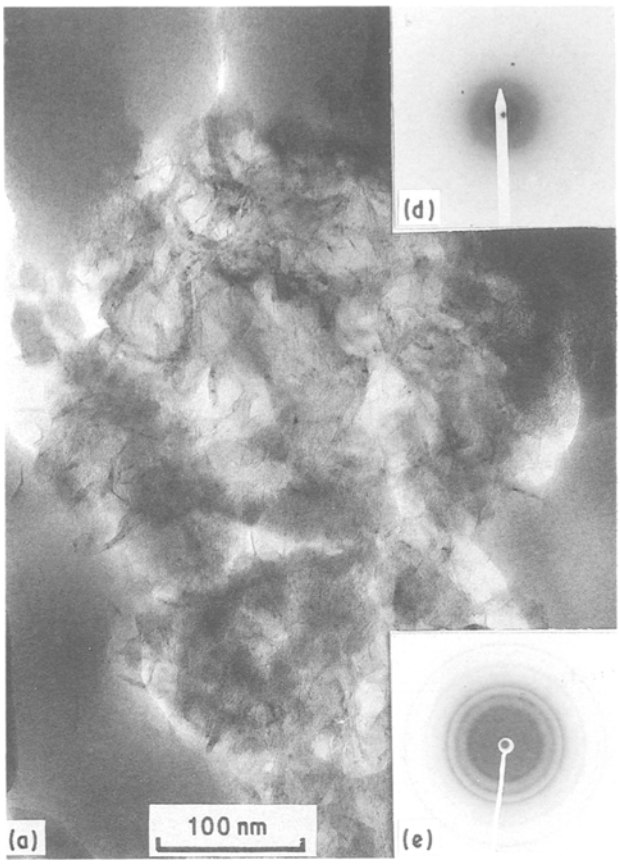

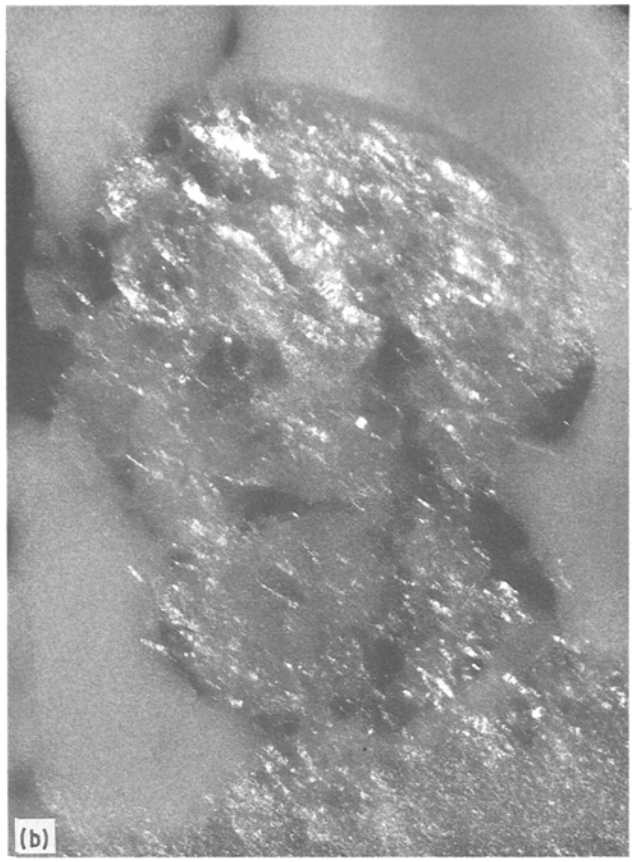

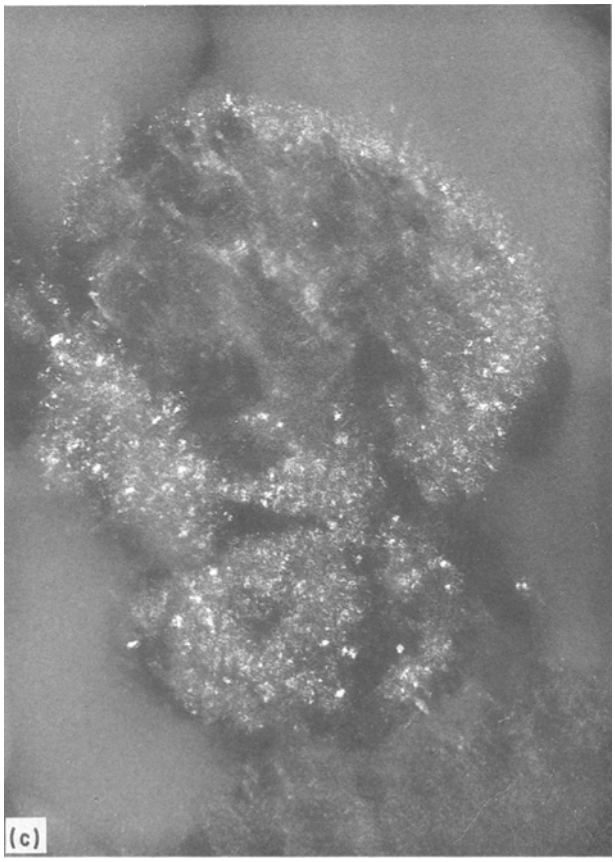

Figure 7 Single filament composite NLP 201–SiC (3 μm thick). Zones 5 and 6. (a) BF; (b) SiO_2–C_{002} DF; (c) SiC_{111} DF; (d) SAD pattern, silica; (e) SAD pattern, nodule.

such a microstructure. Thus catalysis phenomena have occurred. It is known [17] that silicon vapour can transform a poorly organized carbon into a better organized carbon.

The following reaction shows this mechanism:

$$Si + (1 - x)C \rightarrow SiC_{(1-x)} \rightarrow Si + C_{perfect}$$

Recalling the thermal decomposition of the SiC crystals in the fibre, we can recognize that the SiC vapour leaving the fibre can reorganize the porous carbon. On the other hand, the silicon vapour can react with traces of oxygen contained in the furnace to form the SiO_2 phase.

In the SiO_2–C–SiC reaction, it is important to notice that the reaction

$$SiO_2 + 3C \rightarrow SiC + \ldots$$

has previously been observed by other authors [11]. Despite the fact that thermodynamic calculation cannot explain the occurrence of this reaction, it may occur easily, as shown in Fig. 7.

In conclusion we may describe the several phenomena occurring during a SiC coating of a fibre.

(a) The SiC crystals of the fibre are degraded into a solid carbon residue. Then labile silicon species may form a silica layer between the fibre and the surface.

(b) The silicon vapour reorganizes the microporous carbon, to form perfect planar aromatic layers.

(c) Complex reactions occur between silica and carbon, to form large SiC crystals.

(d) The vapour phase coming from the furnace finally induces deposition of an SiC matrix. The orientation of this matrix is not perfect, due to the fact that the carbon–SiC substrate has no preferred orientation.

4.3. Thin SiC coating

This sample will not be wholly described here. Nevertheless an interphase has grown. This interphase is made of porous carbon and silica.

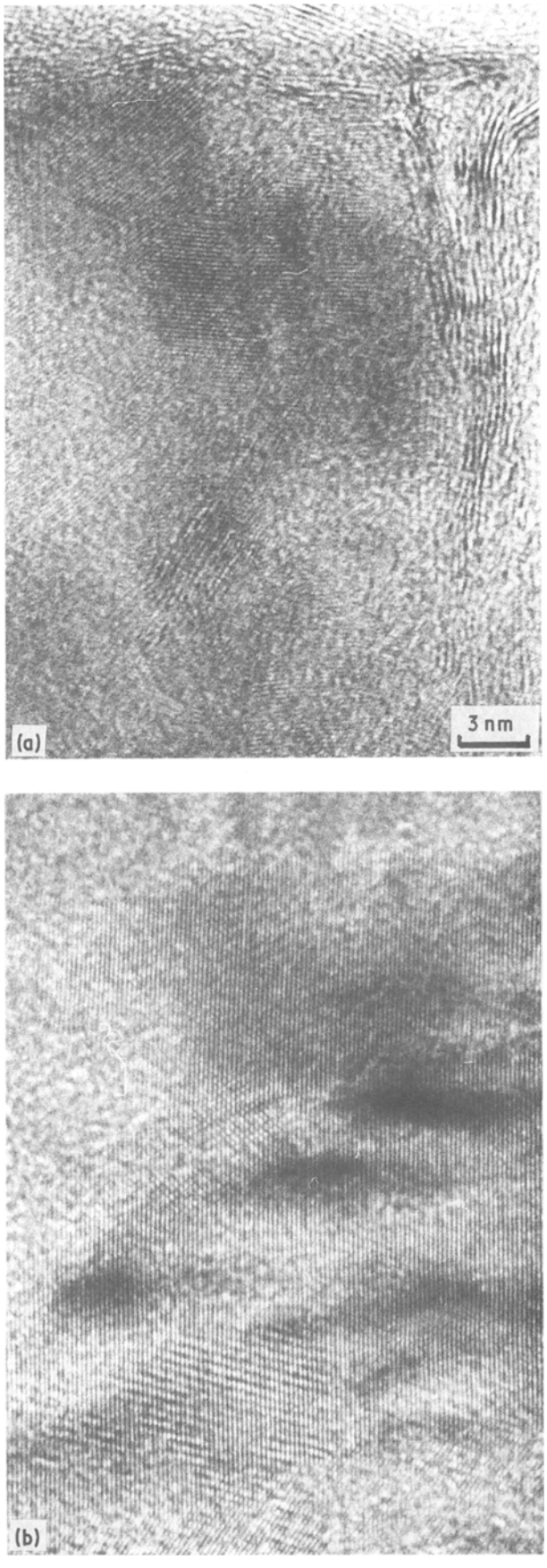

Figure 8 Single-filament composite NLP 201–SiC (3 μm thick). (a) LF zone 7, (b) LF zone 8.

4.4. Thick carbon coating (2 μm)

As in the former cases, an interphase exists between the fibre and the pyrocarbon matrix. This interphase is made of two zones. Fig. 9 shows the interphase, zones 1 and 4 are the fibre (1) and the coating (4).

4.4.1. Description of the interphase

Zone 2 appears in Figs 8a to c Fig. 8a is a SiC_{111} DF. A major crystallization of SiC appears in this zone. The crystal size can be up to 100 nm and Bragg fringes are present. The SAD pattern of this zone (Fig. 9d) shows that it is made of β-SiC mixed with carbon. The carbon may be seen in the Figs 9b and c DF. It is made of short stacks. The LF micrograph of Fig. 10a shows a representative feature recorded in this area. No noticeable orientation relationship exists between SiC crystals and carbon planes.

Zone 3 is visible in Figs 9b and c SiO_2–C_{002} DF. Two phases are contained in this zone. First, carbon layer stacks appear in the shape of long bands, which are visible in both the micrographs. Thus no orientation exists regarding this carbon but it is well organized. Second, amorphous silica is present in the shape of large greyish areas (arrow). Fig. 10b (LF micrograph) shows the peculiar shape of carbon layer stacks in this zone in contact with the carbon deposit. The fringes are straight and their length has increased up to 100 nm. This peculiar texture should be compared with that of the pyrocarbon matrix shown in Fig. 10c which is characteristic of a low-temperature pyrocarbon. The local misorientation ($\pm 45°$) is relatively small, as it is also seen in the SAD patterns (insert Fig. 10b). However, in some places, the local misorientation may reach 180°.

4.4.2. Discussion

As in the case of the former sample, the existence of a thick interphase has been proven, and as in SiC-coated fibre, this interphase is a double interphase. The first part of this interphase is near the fibre (zone 2) contain-ing both carbon and SiC. The second part of the interphase (zone 3) is mainly constituted of amorphous silica, as in the former samples. Nevertheless, carbon is also present, shaped in long perfect stacks.

The presence of this double interphase can be explained by remembering the thermal degradation of the fibre. The SiC crystals of the fibre decompose and a silicon-containing vapour phase leaves the fibre surface. This gaseous phase may form a silica layer (zone 3). On the other hand, silica can react with excess carbon species emanating from the surface and forms large SiC crystals. They partly decompose into carbon and silicon-containing vapour which may include a catalytic transformation of the carbon just before the pyrocarbon deposit occurs. The catalytic carbon is made of long straight and perfect fringes following the reaction

$$Si + (1 - x)C \rightarrow SiC_{1-x} \rightarrow Si + (1 - x)C_{perfect}$$

4.5. The thin carbon coating (0.4 μm)

Owing to the small thickness of the coating, no true interphase has been found in this sample. A very thin layer of porous carbon may be found between the fibre and the pyrocarbon matrix.

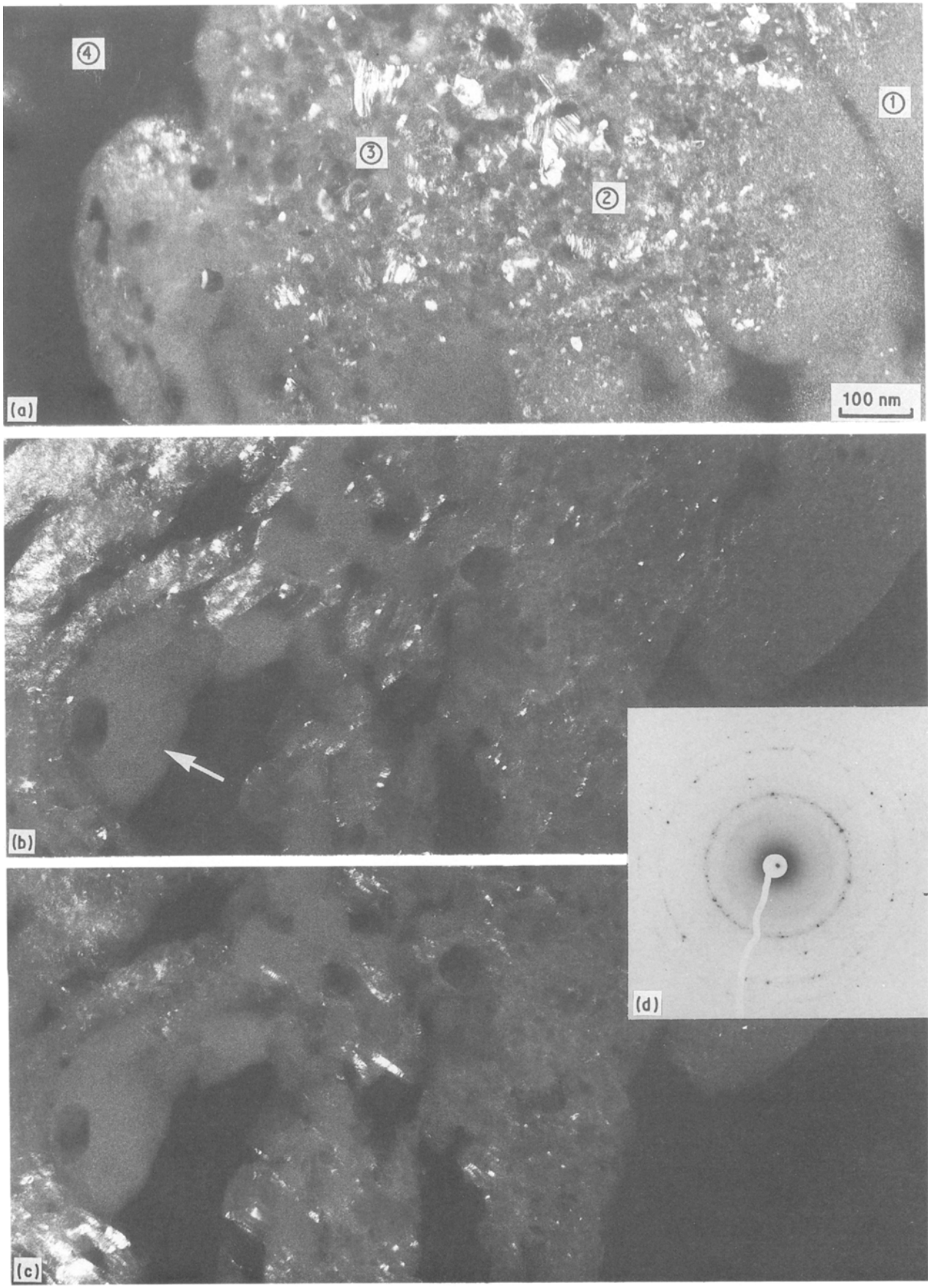

Figure 9 Single-filament composite NLP 201–carbon (2 μm thick). (a) SiC_{111} DF; (b) and (c) orthogonal SiO_2–C_{002} DF; (d) SAD pattern of zone 2.

5. Discussion

The thermal degradation of the Nicalon fibres has been explained through this study. The small SiC crystals decompose by losing labile silicon species and a solid carbon residue remains. This residue is porous and poorly organized. The carbon diffraction units are small in size because the SiC crystals from which they issue are themselves small. The silicon species were

oxidized and formed amorphous SiO_2 as an external layer. The corrosion of the fibre due to the residence time in the furnace during the CVD process is the origin of all the interphases observed, depending on which coating is used.

In the case of SiC coating, the labile reactive silicon issued from the fibre diffuses through the badly organized carbon. It can thus react with it so as to form large perfect carbon layer stacks visible in projection as long straight bands. A reaction previously reported by other authors (9–11, 17) explains this phenomenon. It leads to meso- and macroporous carbon interphases.

The labile silicon phase combines with the oxygen in the furnace to form SiO_2. This amorphous phase cannot be stable in the presence of excess carbon species and silica is destroyed to form SiC again. The partial subsequent decomposition of SiC then forms layers of catalytic carbon. It is these two phenomena which are predominant in the case of carbon coatings. These relatively simple reactions explain the paradoxical results obtained:

(i) in the case of SiC deposits the interphase first obtained are only carbon and silica;

(ii) in the case of carbon deposits the interphases obtained are only carbon and SiC.

Inside the core of the fibre no change occurs except for an increase in the size of the SiC crystal due to kinetics effects and the improvement in free-carbon organization. Apparently no effect can be expected from the SiOC grain boundaries between SiC crystals, because at a temperature below 1400° C even for long residence times, no release is detected by elemental analysis.

Acknowledgements

The authors thank DRET and the Société Européenne de Propulsion (SEP) for supporting this study.

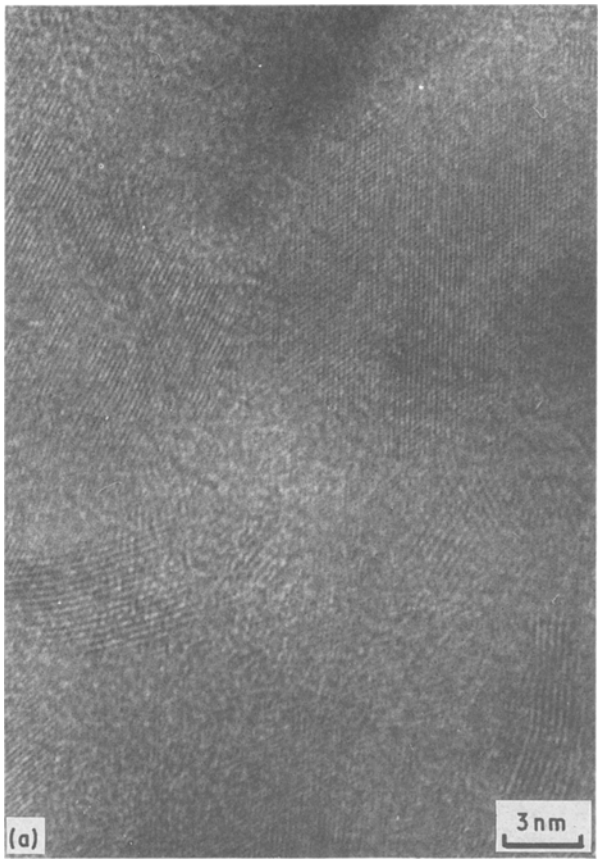

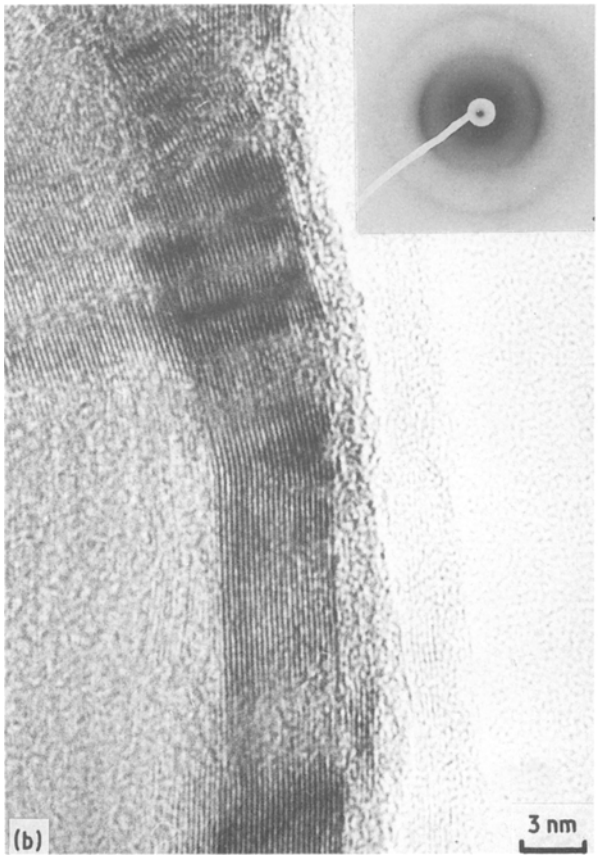

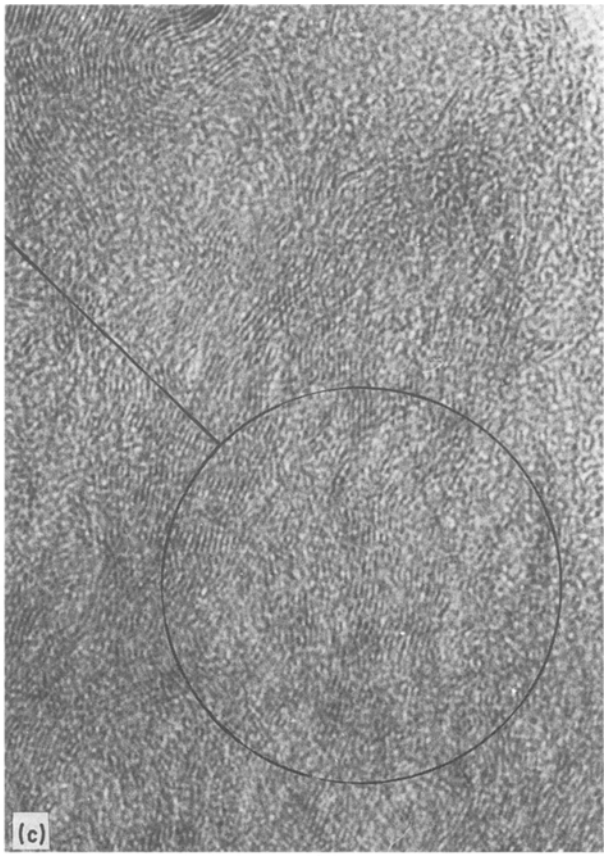

Figure 10 Single-filament composite NLP 201–carbon (2 μm thick). LF micrographs of (a) zone 2; (b) zone 3, inset SAD pattern of zone 4; (c) zone 4.

References

1. L. HERAUD, Contract report DRET 84 445 (1986).
2. Y. MANIETTE, *J. Mater. Sci. Lett.* **9** (1990) 48.
3. J. AYACHE, S BONNAMY, X. BOURRAT, A. DEURBERGUE, Y. MANIETTE, A. OBERLIN, E. BACQUE, M. BIROT, J. DUNOGUES and J. P. PILLOT, *ibid.* **7** (1988) 885.
4. Y. MANIETTE and A. OBERLIN, *J. Mater. Sci.* **24** (1989) 3361.
5. M. MONTHIOUX and A. OBERLIN, *Composite Sci. Technol.*, **37** (1990) 21.
6. Y. MANIETTE, Thesis, Univesité de Pau, December 1988.
7. P. CHAUDHARI, *Phys. Status. Solidi* **51** (1972) 801.
8. R. HAGEGE, P. OLRY, J. COTTERET, M. LARIDJANI, J. DIXIMIER, C. LAFFON, A. M. FLANK, P. LAGARDE, J. L. MIGUEL, H. HOMMEL and A. P. LEGRAND, *J. Mater. Sci.* **24** (1989) 1503.
9. D. F. BADAMI, *Carbon* **3** (1955) 53.
10. A. ADDAMIANO, in "Silicon Carbide" (University of S.C. Press, 1977) p. 179.
11. A. OBERLIN, M. OBERLIN and J. R. COMTE TROTET, *J. Microsc. Spectrosc. Electr.* **1** (1976) 391.
12. S. IIJIMA, *J. Solid State Chem.* **42** (1982) 101.
13. L. MUELHOFF, W. J. CHOYKE, M. J. BOZAK and J. T. YATES Jr, *J. Appl. Phys.* **60** (1986) 2848.
14. A. OBERLIN, unpublished results.
15. F. D. RICHARDSON and J. H. E. JEFFES, *J. Iron Steel Inst.* **160** (1948) 261.
16. C. H. ANDERSSON and R. WARREN, *Composites* **15** (1984) 16.
17. J. GILLOT, W. BOLLMANN and B. LUX, *Ber. Deut. Keram. Ges.* **45** (1968) 224.

Received 4 July
and accepted 29 September 1989